MEASUREMENT OF SURFACE AND INTERFACIAL TENSION BASED ON THE PENDANT DROP METHOD

Fabiano G. Wolf, fgwolf@lmpt.ufsc.br
Weliton Hodecker, weliton@lmpt.ufsc.br
Giuseppe S. Zanella, giuseppe@lmpt.ufsc.br
Paulo C. Philippi, philippi@lmpt.ufsc.br
Federal University of Santa Catarina, Department of Mechanical Engineering, Porous Media and Thermophysical Properties Laboratory, Campus Universitário, Florianópolis, Santa Catarina 88040-900, Brazil

Abstract. *The development of a computational method for the measurement of surface and interfacial tension based on the pendant drop method is presented. The method is based on the analysis of the picture of a suspended drop, whose geometrical shape can be described by the Young-Laplace equation. A new method for edge detection with sub-pixel resolution is discussed for grayscale images and the Generalized Simulated Annealing method is used for the minimization of the objective function. Experiments were performed for common pure liquids and the experimental results were compared with those found in the literature.*

Keywords: *surface and interfacial tension, pendant drop method, edge detection with sub-pixel resolution, Generalized Simulated Annealing*

1. INTRODUCTION

Surface phenomena are important for a wide range of scientific areas, such as physics, chemistry and engineering. Most of them involve the interaction of different fluid phases that are put together to form an interface, whose physical behaviour can be quantified by the value of the surface tension. Some usual industrial applications are emulsification, coating, painting, lubrication and oil recovery. A common technique used to measure surface and interfacial tension is the pendant drop method [1, 2]. The pedant drop method is based on the analysis of a suspended drop on a needle or capillary tube. Its popularity is due to the requirement of small quantities of liquids and its applicability to many experimentally difficult situations of measurement, e.g., such as time, pressure and temperature dependence [3]. In this work, the development of a computational application for measuring surface and interfacial tension by using the pendant drop method is presented, including a new method for edge detection with sub-pixel resolution for grayscale images. Furthermore, the Generalized Simulated Annealing method [4, 5] was used for the minimization of the objective function which describes the deviation between the theoretical and experimental drop profiles.

2. THE PENDANT DROP METHOD

2.1 Theoretical background

The pendant drop method [1, 2] is based on the analysis of the drop profile of an axisymmetric drop on the tip of a capillary tube. Under hydrodynamic equilibrium conditions, the gravity force on the drop is counterbalanced by the surface force, defining a physical configuration that can be described by a special form of the Young-Laplace equation, known as Bashforth-Adams equation [6]. The pendant drop method can be outlined by the following steps: (i) image processing using an edge detection algorithm and extraction of the drop profile on a suitable coordinate system; (ii) determination of the system resolution and coordinates of the drop apex; (iii) estimation of the shape parameter and capillary length; (iv) minimization of the objective function which represents the deviation between the experimental and theoretical drop profiles. The surface tension is determined after the best fitting of the experimental and theoretical profiles to be reached, in step (iv), in which the theoretical equivalence of the experimental drop is found.

By considering the coordinate system $x-z$ displayed in Fig. 1, in which the coordinate point (x, z) of the drop profile is written in terms of the arc length s measured from the origin O, the Bashforth-Adams equation [6] can be represented in dimensionless form by the following equations [7, 2]:

$$\begin{aligned} \frac{d\phi}{dS} &= \frac{2}{B} - Z - \frac{\sin\phi}{X}, \\ \frac{dX}{dS} &= \cos\phi, \\ \frac{dZ}{dS} &= \sin\phi, \end{aligned} \tag{1}$$

where $X = x/a$, $Z = z/a$, $S = s/a$, $B = b/a$ and ϕ is the angle between the tangent line to the interface at the point

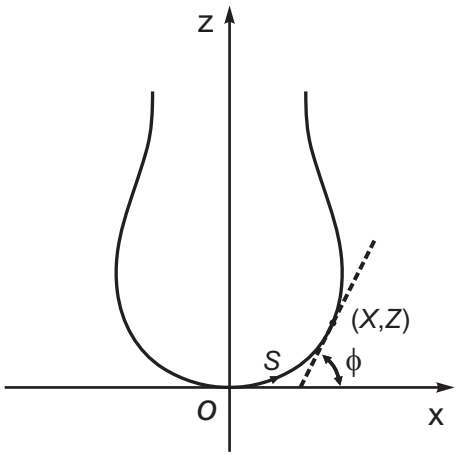

Figure 1. Coordinate system for the pendant drop.

(x, y) and the axis x. In the equations above, B is the shape parameter, b is the curvature radius at the drop apex and a is the capillary length given by

$$a = \sqrt{\frac{\gamma}{\Delta\rho g}},$$

where γ, $\Delta\rho$ and g are the surface tension, the density difference between the phases and the gravity, respectively.

Equations 1 with the boundary conditions at the drop apex, $X(0) = Z(0) = \phi(0) = 0$ and $\sin\phi/X(0) = 1/B$, form a set of first order differential equations and can only be solved by numerical procedures. In this work, the fourth order Runge-Kutta scheme [8] was used for this purpose. Some numerical solutions for Eq. 1 for different shape parameters are shown in Fig. 2.

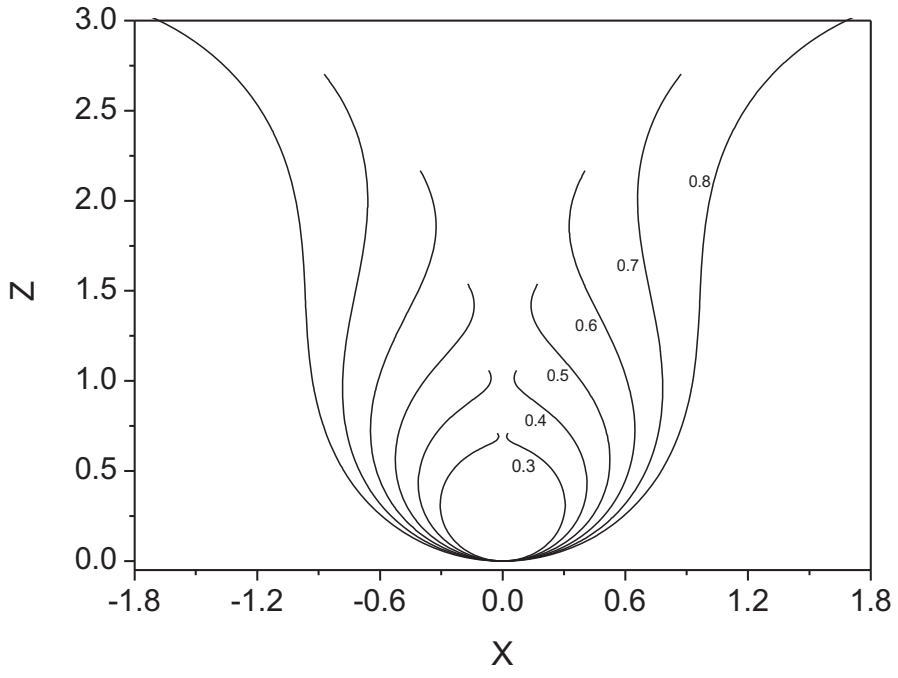

Figure 2. Solutions of the dimensionless Bashforth-Adams equation as a function of shape parameter.

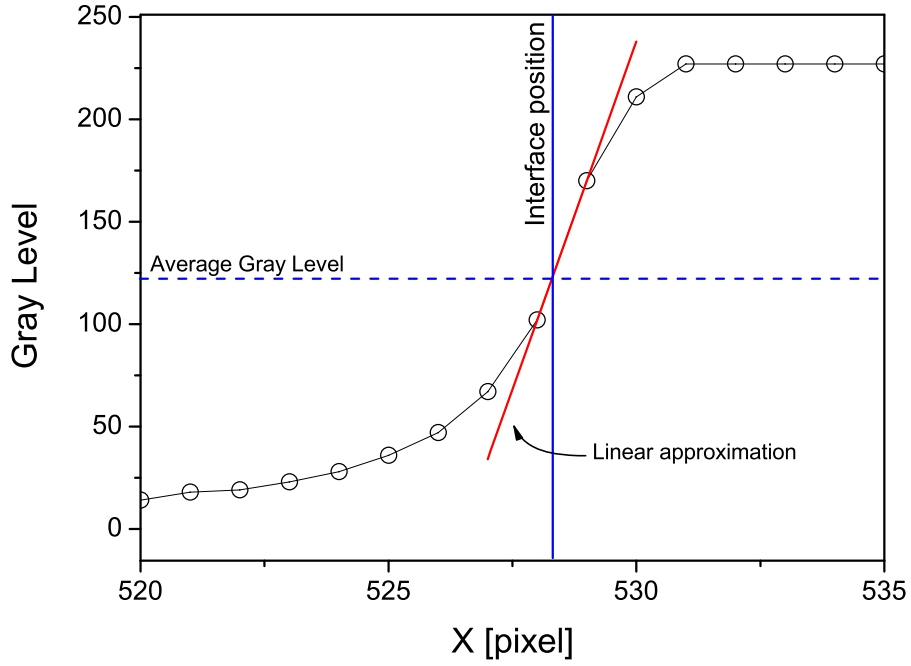

Figure 3. Schematic illustration of an interfacial region and the linear interpolation defining the interface position with sub-pixel resolution.

2.2 Edge detection with sub-pixel resolution

The pendant drop method analyzes the shape of the drop using image processing and calculates the associated surface tension. For this, it needs an efficient method to recognize and extract edges from a grayscale image, since the numerical precision of the coordinate points which make the drop profile is essential for accuracy of the value of surface tension. In this work, the acquisition of images has been done by a goniometer provided by DataPhysics Instruments GmbH. Such equipment makes possible the capture of grayscale pictures with size of 768×574 pixels. The drop profile, which is the set of coordinate points related to an appropriated coordinate system, was obtained according to the following numerical procedure:

(i) The Sobel operator [9] with a grid of 3×3 pixels was applied to the image for calculating the graylevel gradient, the *local* slope of the gradient – which defines the interface orientation to one of the main directions, represented by the angles $0°$, $45°$, $90°$ and $135°$ –, and the maximum, $\max |G|^{global}$, and minimum, $\min |G|^{global}$, gradients of the image;

(ii) The pixels satisfying the following threshold are considered part of the interface (with pixel resolution):

$$\max |G|^{local} > \alpha \left(\frac{\max |G|^{global} + \min |G|^{global}}{2} \right) \tag{2}$$

where $\alpha = 0.8$ and the *local* maximum gradient, $\max |G|^{local}$, is determined according to the interface orientation for a grid of 11×11 pixels. In sequence, the non-maximum suppression is applied, in which any pixel value that is not considered to be an edge is suppressed, i.e., if a pixel does not satisfy the above condition, Eq. 2, it is removed before the subsequent analysis;

(iii) After those pixels representing an interfacial area are defined, it is assumed a linear interpolation for the graylevel variation perpendicularly to the interface, defining the interface position by the mean graylevel, determined from the maximum and minimum graylevel values in a grid of 11×11 pixels. This enables the calculation of the interface position with sub-pixel resolution, as displayed schematically in Fig. 3.

A drop profile built according to the steps above is shown in Fig. 4.

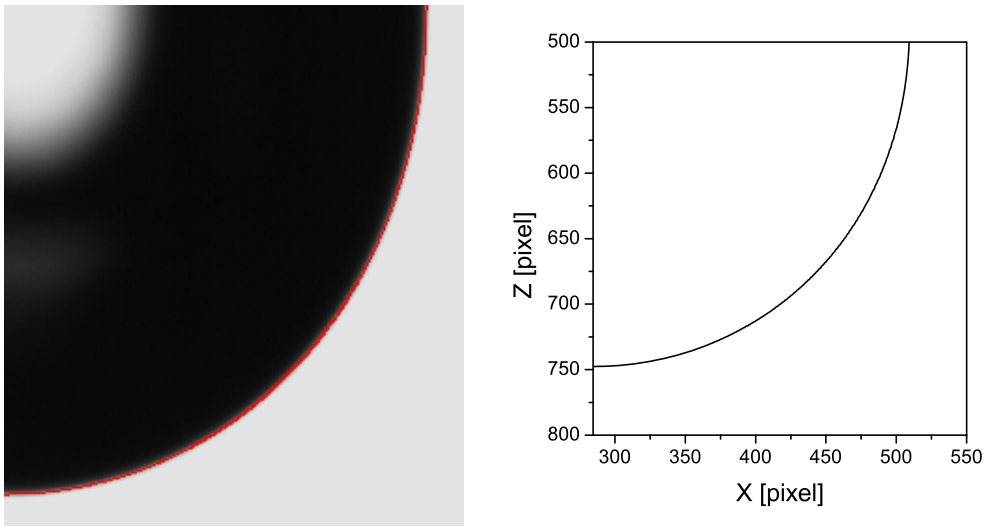

Figure 4. A grayscale image and resulting drop profile achieved after applying the edge detection algorithm. Those red pixels on the interfacial region in the grayscale image represent the drop profile with pixel resolution, while the profile on the right was obtained with sub-pixel resolution.

2.3 Mean drop profile, system resolution and apex coordinates

The Bashforth-Adams equation [6] presupposes that the profile of pendant drop is axisymmetric, so that just one of the sides of drop needs to be analyzed. However, it is very difficult to get pendant drops that are perfectly aligned, given the difficulty in achieving an ideal alignment between the vertical axis of the acquisition camera and the vector of gravity. A plumb line can be used to minimize such problem. Furthermore, sometimes it is necessary to fix or minimize *small* tilting effects of the drop, because well elaborated and accurate experiments can take a long time to be concluded. The implemented method for minimizing the problem is based on the mean drop profile between the right and left drop sides by taking the coordinates of the drop apex into account, (x_0, z_0), as the reference. The mean profile is calculated following the same way used by Song and Springer [2]:

$$x_m(z) = x_0 + \frac{x_R(z) - x_L(z)}{2} \tag{3}$$

where $x_L(z)$, $x_R(z)$ and $x_m(z)$ represent the coordinate *x* of drop on the right and left sides and the mean profile, respectively. The determination of the coordinates of drop for any component *z* was performed by applying third order interpolations. The coordinates of the apex drop, (x_0, z_0), were calculated previously by second order interpolations applied to the lowest part of the pendant drop.

Another important quantity in the pendant drop method is the system resolution, i.e., the physical scale that represents each pixel of the image. A very convenient way to determine that parameter comes from the own needle used to produce the drop, because the needle can also be photographed in the process. From the external diameter of the needle, which can be measured by a micrometer, one can determine precisely the physical resolution of the system. The algorithm used in Section 2.2 for detecting the drop profile was also used to determine the external diameter in pixel units.

2.4 Estimation of the shape parameter and capillary length

As seen previously, the dimensionless form of the Young-Laplace equation mentioned above can be solved as a function of shape parameter, B. A good estimate for this parameter is obtained from the geometrical dimensions of the pendant drop. Defining two characteristic values of diameter, the equatorial diameter, D_E, measured in the largest section of the drop and the second diameter, D_S, measured in that section separated by a vertical distance D_E far from the drop apex, as shown in Fig. 5, one can calculate the shape parameter by the Huh and Reed relationship [10]:

$$B^2 = \exp\left(-6.70905 + 15.3002S - 16.4479S^2 + 9.92425S^3 - 2.58503S^4\right),$$

where $S = D_S/D_E$. Third order interpolations were used for measuring D_E and D_S in an appropriate way.

After obtaining B, which characterizes the physical relationship between the capillary and gravity forces, it is necessary to determine the capillary length, which gives the characteristic surface tension of the liquid-gas system under study. The capillary length, a, was determined by the least-squares method combined with the shape comparison method [11]. The shape comparison method consists in finding the coordinate points in both experimental and theoretical profiles that

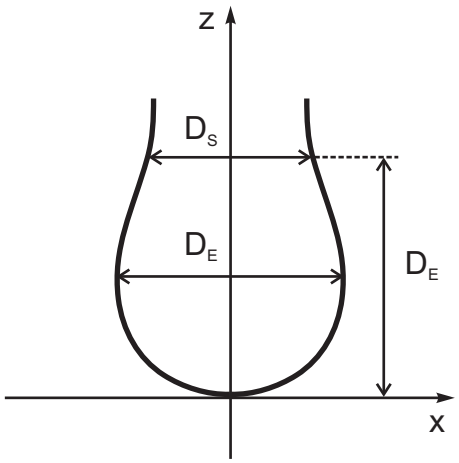

Figure 5. Schematization of the characteristic values of diameter in the Huh and Reed formula [10].

are geometrical comparable. In this way, the capillary length is estimated by the following relationship:

$$a = \frac{\sum_{i=0}^{N-1} Z_i \left(z_i - z_0\right) + \sum_{i=1}^{N} X_i \left(x_i - x_0\right)}{\sum_{i=1}^{N} Z_i^2 + \sum_{i=1}^{N} X_i^2}, \tag{4}$$

where N is the number of points of the experimental profile and (X_i, Z_i) represents the theoretical coordinate that is geometrically comparable to the experimental coordinate (x_i, z_i). The calculation of a by Eq. 4 enables an initial estimation of surface tension, whereas the capillary length is defined by $a = \sqrt{\gamma/\Delta\rho g}$. Such definition takes into account the high-precision measurement of the density difference and the local gravity, so that a reliable value of surface tension is obtained.

In order to decrease the demanding time for this process, only 5% of the experimental points are considered, resulting, typically, around 50 coordinates. Such procedure does not represent any limitation, because a small number of accurate points is already enough for the accuracy of the surface tension calculation [1].

2.5 Optimization of the drop profile

The method used in Sec. 2.4 provides a good estimation of surface tension for a given physical system. However, it is possible to improve the solution through a minimization process of the objective function, $E = E\left(B, a, x_0, z_0, \theta, \mathcal{R}\right)$, which represents the deviation between the experimental and theoretical profiles, where θ is the tilted angle of the drop with respect to the coordinate system and $\mathcal{R}$ is the pixel aspect ratio resulting from the electronic system used for the image acquisition, defined as the ratio between the width and height of the pixel. Such minimization process seeks for the global minimum of the objective function, requiring some numerical techniques of optimization. In this work, the Generalized Simulated Annealing method (GSAM) [12, 5, 4] was implemented for the purpose of minimizing the function E, defined here by the root mean square residual:

$$E = \frac{1}{N} \sum_{i=0}^{N-1} \sqrt{\left[\left(x_i - x_0\right) - \left(X_i \cos\theta - Z_i \sin\theta\right) a\right]^2 + \left[\left(z_i - z_0\right) - \left(X_i \sin\theta + Z_i \cos\theta\right) a\right]^2}, \tag{5}$$

where (x_i, z_i) and (X_i, Z_i) are the coordinates of the experimental and theoretical profiles that are comparable geometrically, as mentioned previously. For simplicity, the optimization of the pixel aspect ratio was not carried out, once that the previous knowledge of $\mathcal{R}$ allowed such correction immediately after the drop profile detection. The implementation of the GSAM was done similarly with the one implemented by Penna [5], who demonstrated the applicability of the GSAM for fitting curves. The algorithm is described briefly bellow.

Let $E(x)$ the function to be minimized, dependent of the variable x. One can evaluate the probability the variable x changing from x_t to x_{t+1}, displaying the variation $\Delta x_t = x_{t+1} - x_t$, following the *visiting* distribution, $g_{q_V}\left(\Delta x_t\right)$, defined as [12, 5]

$$g_{q_V}\left(\Delta x_t\right) \propto \frac{T(t)^{-\frac{D}{3-q_V}}}{\left[1 + \frac{(q_V - 1)(\Delta x_t)^2}{T(t)^{\frac{2}{3-q_V}}}\right]^{\frac{1}{q_V - 1} + \frac{D-1}{2}}},$$

where q_V is the visiting parameter, D is the dimension of the function to be minimized and $T(t)$ is an artificial temperature at the time t given by

$$T(t) = T(1)\frac{2^{q_V-1}-1}{(1+t)^{q_V-1}-1}.$$

As a conventional minimization method, every time the variation Δx_t leads to a decrease in the objective function, i.e., if $E(x_{t+1}) < E(x_t)$, the new value of x will always be accepted. On the other hand, if that variation leads to an increase or no change in the objective function, i.e., if $E(x_{t+1}) \geq E(x_t)$, that variation will be accepted according to an *acceptance* probability, $P(x_t \rightarrow x_{t+1})$. The acceptance probability can be written as [5, 4]

$$P(x_t \rightarrow x_{t+1}) = \begin{cases} 1, & \text{if } E(x_{t+1}) < E(x_t) \\ \dfrac{1}{\left[1+(q_A-1)\frac{E(x_{t+1})-E(x_t)}{T(t)}\right]^{\frac{1}{q_A-1}}}, & \text{if } E(x_{t+1}) \geq E(x_t), \end{cases}$$

where q_A is the acceptance parameter.

In this work, the adopted procedure for the minimization of Eq. 5 was based on the running of the algorithm described above for $t = 1..500$ during 50 trials, attributing the initial value of E, at each new trial N, the minimum value of E found at the previous trial $N-1$, i.e., $E_N(t=1) = \min E_{N-1}$. The values $q_V = 1.7$ and $q_A = -5.0$ were chosen for the solution of the problem under study.

3. MATERIALS AND METHODS

The reported experiments were carried out with a goniometer, model OCA20, provided by DataPhysics Instruments, connected to a computer. Glass syringes and stainless steel needles with external diameter of 0.908 ± 0.001 and 1.652 ± 0.001 mm were used. The measurement of surface tension is strongly affected by contaminants in the environment. Minimizing such problems is vital for the correctness of the measured values. In this way, the glassware and needles was basically cleaned by mechanical washing with detergent and water, followed by an immersion in solution of 10% KOH in ethanol and aqueous solution of 10% HNO_3, ultrasonic cleaning, rinsing with deionized and distilled water, and drying at 80 °C. Some common liquids were used in the measurements and their physical-chemistry properties are shown in Tab. 1.

All the experiments were performed at the temperature of 20 ± 0.5 °C. Each value of surface tension was determined from the mean value of N independent drops. Each drop picture was taken after the mechanical equilibrium of curvature was observed, occurring, typically, between 10 and 60 seconds. Additionally, the surface tension of each liquid was also measured by the Wilhelmy plate technique [13] by using a conventional tensiometer, model Sigma 700, provided by KSV Instruments, and represented by γ_{WP}. For Ethanol and Acetone, it was observed that the liquid wets strongly on the outside surface of the needle, avoiding the correct formation of axisymmetric drops. In these cases, a layer of hydrophobic coating, provided by Dataphysics Instruments, was applied to the needle tips.

4. RESULTS AND DISCUSSION

The physical-chemistry properties of some common liquids, for which the surface tensions were measured in present experiments, are listed in Tab. 1, where the values of surface tension available in the literature are represented by γ_l. Experimental values that were obtained in the laboratory with a tensiometer KSV, model Sigma 700, are symbolized by γ_{WP}. The obtained results with the pendant drop method are shown in Tab. 2, Figs 6 and 7.

Figure 7 displays the coordinate points and the best-fitted theoretical curve for each drop. As can be seen, the optimization method was efficient in fitting the best theoretical drop to each set of experimental points. The obtained results for the estimation performed by the least-squares method is also displayed in Tab. 2 for comparison, since it offers a simple and fast calculation method.

The statistical error in the confidence interval of 95% was observed to be small in most of the results, and can be attributed to the accuracy of the edge detection method developed in this work. In the case of Acetone, such error is larger, considering its high volatility, which made difficult the definition of a static liquid-gas interface during the experiment.

Noticing that most of the measuring methods in liquid-fluid systems do not provide an accuracy better than around 0.1 mN/m [14], the measured values of surface tension are to be considered as satisfactory. Errors between the values found in the literature and the measured ones, E_l, were small, even though when the statistical analysis was carried out with a low number of independent drops.

The observed discrepancies can be due to impurities in the air, and to the assumption of the air density to be a constant, 0.0012 g/cm^3, in all experiments. The latter is particularly incorrect for volatile liquids, like alcohols and Acetone, because the true density in such cases must comprises the mixture between air and liquid vapor. In the presence of contaminants, a better control of the surrounding atmosphere by using an inert gas, like Argon, would be appropriate. Regarding the reference [18], it is observed a high deviation for Isopropanol with respect to the measured surface tension, also verified

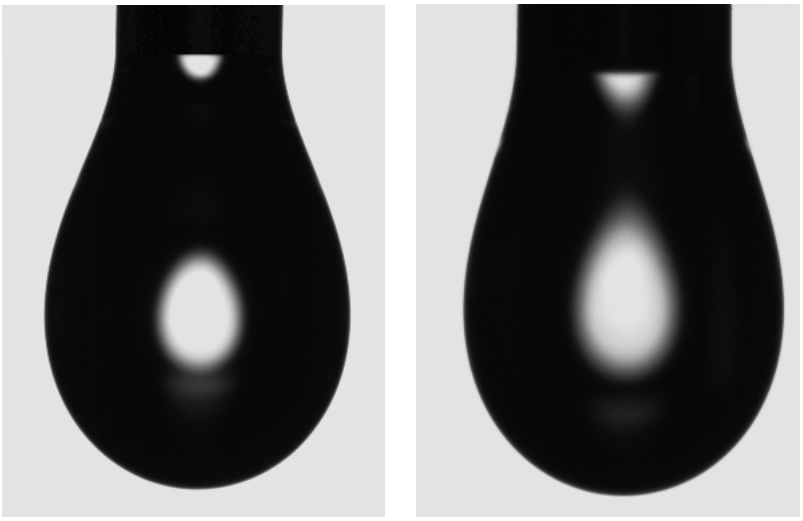

(a) Formamide. (b) Acetone.

Figure 6. Drop pictures analyzed in the experiments. In both pictures the external diameter of the needle is 1.652 ± 0.001 mm.

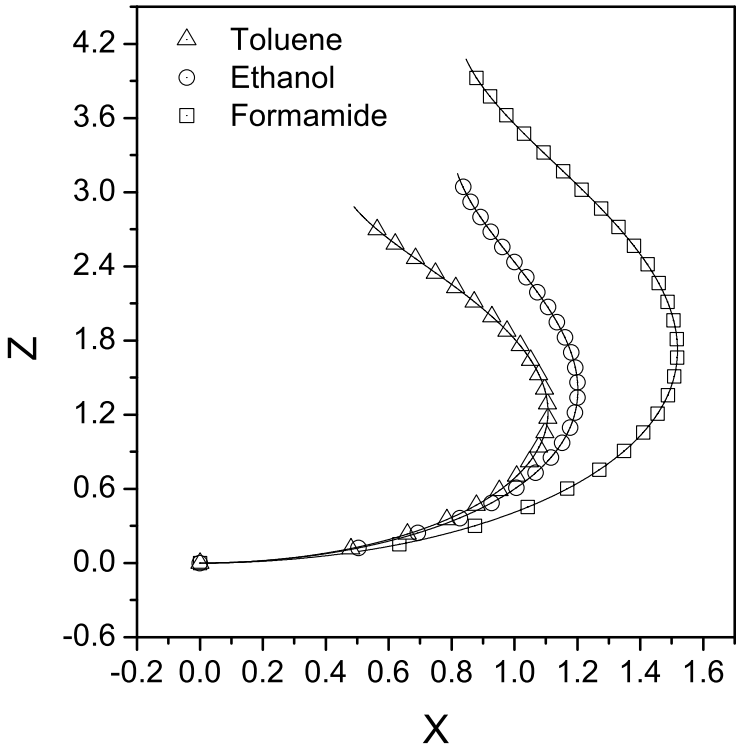

Figure 7. Experimental and best-fitted theoretical drop profiles.

Table 1. Physical-chemistry properties of some liquids found in the literature at the temperature 20 °C.

Liquid	$\rho\ [g/cm^3]$	Purity [%]	$\gamma_l\ [mN/m]$	$\gamma_{WP}\ [mN/m]$	Reference
Formamide	1.1334	99.0	58.20	58.21	Chen and Wakida (1997) [15]
Toluene	0.8670	99.5	28.52	28.49	Adamson (1990)[16]
Ethanol	0.7894	99.5	22.39	22.36	Adamson (1990)[16]
Isopropanol	0.7875	99.5	21.32	21.03	Speight (2005)[17]
			23.05		Yaws (1999)[18]
Acetone	0.7844	99.5	24.02	23.70	Speight (2005)[17]

Table 2. The obtained results with the pendant drop method in the confidence interval of 95%. The air density and acceleration of gravity were assumed to be constant and equal to 0.0012 g/cm ^{3} and 9.791 m/s, respectively.

Liquid	N	B	$a[mm]$	$\gamma[mN/m]$	$E_l[\%]$	$\gamma_{LSF}[mN/m]$	$E_{LSF}[\%]$
Formamide	12	0.614	2.295	58.40±0.06	0.3	58.45±0.07	0.4
Toluene	12	0.568	1.832	28.45±0.05	0.2	28.55±0.03	0.1
Ethanol	8	0.644	1.706	21.98±0.03	1.8	22.00±0.03	1.7
Isopropanol	9	0.659	1.656	21.06±0.02	1.2	21.12±0.02	0.9
					8.6		8.4
Acetone	12	0.644	1.758	23.70±0.10	1.3	23.73±0.09	1.2

by the Wilhelmy plate technique. As both measuring methods used in this work showed similar deviations with respect to that tabulated value in reference [18], we conclude that the experimental conditions imposed in our experiments were different those found in the mentioned citation. In general, the least-square method provided comparable results with respect to the minimization method. The implemented minimization method in Sec. 2.5 reduced the root mean square residual, E, between the experimental and theoretical profiles, on average, from 2×10^{-3} mm to 5×10^{-4} mm, i.e., around 75%. Anyway, the measured values of surface tension did not change significantly, showing that the objective function, Eq. 5, was already close to the global minimum.

5. CONCLUSIONS

A comparison between the obtained results and those found in the literature showed that the developed method, which utilizes image analysis and the pendant drop method, provided satisfactory results for the values of surface tension of pure liquids. Some measured values of surface tension are considerably different from other references, imposing the use of an independent measurement technique. This allowed to recognize that more appropriate control of the surrounding atmosphere can be necessary for high precision values of surface tension. Furthermore, the measurement of the air density of the surrounding phase can improve the obtained results, since the accuracy of the density difference of the involved phases is vital for the calculations. The implemented least-square method gives good estimates for the surface tension, avoiding a minimization method for the objective function.

6. ACKNOWLEDGMENTS

Financial support was given by CENPES/Petrobras, Financial Supporter of Studies and Projects (FINEP) and National Council for Scientific and Technological Development (CNPq).

7. REFERENCES

P. Cheng and A. W. Neumann. Computional evaluation of axisymmetric drop shape analys-profile (adsa-p). *Colloids and Surfaces*, 62:297–205, 1992.

B. Song and J. Springer. Determination of interfacial tension from the profile of a pendant drop using computer-aided image processing. 1. Theoretical. *Journal of Colloid and Interface Science*, 184:64–76, 1996.

P. Cheng, D. Li, L. Boruvka, Y. Rotenberg, and A. W. Neumann. Automation of axisymmetric drop shape analysis for measurements of interfacial tensions and contact angles. *Colloids and Surfaces*, 43:151–167, 1990.

C. Tsallis and D. A. Stariolo. Generalized simulated annealing. *Physica A*, 233, 1996.

T. J. P. Penna. Fitting curves by simulated annealing. *Computers in Physics*, 9:3, 1995.

S. Bashforth and J. C. Adams. *An Attempt to test the Theory of Cappillary Action*. Cambridge University Press and Deighton, Bell and Co, London, 1882.

S. Hartland and R. W. Hartland. *Axisymmetrical Fluid-Liquid Interfaces*. Elsevier, 1976.

Cláudio Scherer. *Métodos computacionais da Física*. Livraria da Física, 2005.
R. O. Duda and P. E. Hart. *Pattern Classification and Scene Analysis*. John Wiley & Sons Inc, 1973.
C. Huh and R. L. Reed. *J. Colloid Interface Sci.*, 91:2, 1983.
S. H. Anatasiadis, J. K. Chen, J. T. Koberstein, A. F. Siegel, J. E. Sohn, and J. A. Emerson. *J. Colloid Interface Sci.*, 119:55, 1987.
D. A. Stariolo and C. Tsallis. *Annual Review of Computational Physics II*. World Scientific, 1995.
K. Holmberg. *Handbook of Applied Surface and Colloid Chemistry*. Wiley and Sons, New York, 2002.
J. Drelich, C. Fang, and C. L. White. *Measurement of interfacial tension in fluid-fluid systems*, pages 3152–3166. Encyclopedia of Surface and Colloid Science. Marcel Dekker, Inc., 2002.
J. Chen and T. Wakida. Studies on the surface free energy and surface structure of ptfe film treated with low temperature plasma. *Journal of Applied Polymer Science*, 63:1733–1739, 1997.
A. W. Adamson. *Physical Chemistry of Surfaces*. Wiley Interscience, New York, 5th edition, 1990.
James G. Speight, editor. *Lange's Handbook of Chemistry*. 16th edition, 2005.
C.L. Yaws. *Chemical Properties Handbook*. McGraw-Hill, 1999.

8. Responsibility notice

The authors are the only responsible for the printed material included in this paper.